NANOPERM-TYPE METALLIC GLASSES STUDIED BY CEMS / CXMS AND NUCLEAR INELASTIC SCATTERING TECHNIQUES

Tomáš Hatala, Marcel Miglierini

Slovak University of Technology in Bratislava, Institute of Nuclear and Physical Engineering, 812 19 Bratislava, Slovak Republic

tomas.hatala@stuba.sk

Received 30 April 2013, accepted 14 May 2013

1. Introduction

Iron-based metallic glasses and their nanocrystalline counterparts are interesting for their high magnetic permeability and remanence. These properties are affected by the alloy's composition and the degree of the crystallization [1]. We have investigated the crystallization properties of $^{57}Fe_{79}Mo_8Cu_1B_{12}$ and $^{57}Fe_{76}Mo_8Cu_1B_{15}$ metallic glasses. The alloys were studied in the as-quenched state and after annealing at 510 and 550 ˚C for 30 min in a vacuum. For a characterisation of the surface crystallization we have used data obtained directly from CEMS (*Conversion electron Mössbauer spectroscopy)* and CXMS (*Conversion X-ray Mössbauer spectroscopy*) measurements. Crystallization in the bulk of the alloys was studied by NIS (*Nuclear Inelastic Scattering*) technique using the 3th generation source of synchrotron radiation.

2. Experimental Details

As-quenched and annealed (to 510 and 550 ˚C) samples were measured by CEMS and CXMS techniques at the *Institute of Nuclear and Physical Engineering, FEI STU.* Using ^{57}Co(Rh) source, they were measured at room temperature. Ribbon-shaped samples were inspected on their wheel and air sides. CEMS and CXMS data provide information from surface regions down to the depth of about 200 nm and 1 000 nm, respectively. For the sake of these experiments, the alloys were prepared from iron enriched to the isotope ^{57}Fe to about 50 %. The natural abundance of ^{57}Fe is only 2.17 %.

The NIS energy spectra were taken at the *ESRF* (*Europe Synchrotron Radiation Facility*) ID 18 beamline at room temperature. Experimental setup of a NIS experimental set-up is shown in Fig. 1.

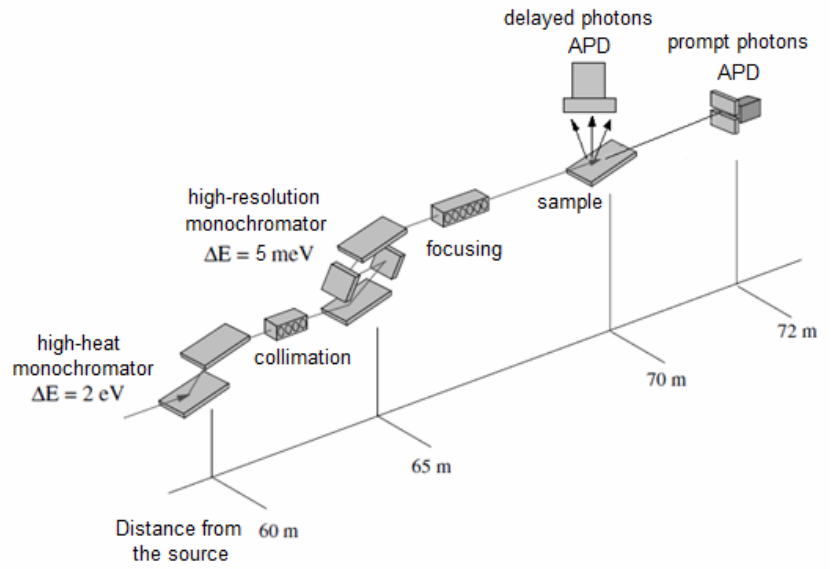

Fig. 1. *Experimental setup of a NIS experiment.*

Synchrotron radiation of high brilliance is created by an undulator and directed to a high-heat load monochromator, through the collimation to a high-resolution monochromator and to the sample, where all nuclear energy levels of ^{57}Fe nuclei are excited at the same time with an energy of 14.413 keV. The deexcitation process is detected by avalanches photodetectors (APD) in two directions. The prompt signal in the forward direction records this particular resonance energy. The second photodetector, positioned perpendicular to the beam propagation direction near the sample's surface, detects delayed fluorescence photons resulted from inelastic scattering. The energy scan is realised by mutual rotation of the planes of the two high resolution monochromators. In our case, they provided energy resolution of about 1 meV. Using this energy window, an energy range from -60 to 80 meV around the reference, i.e. the resonance energy of 14.413 keV was inspected.

3. Results

Figure 2 shows CEMS and CXMS spectra obtained from the wheel side and the air side of the $^{57}Fe_{79}Mo_8Cu_1B_{12}$ ribbons. As stated above, the CEMS and the CXMS data scan different depths regions under the surface. Therefore we see different amounts of amorphous and nanocrystalline structural components. The nanocrystalline phase (dark grey in Fig. 2) consists of a wide distribution of magnetic hyperfine fields and narrow six-line subspectra. They describe interfacial regions and bcc-Fe crystals, respectively. The former represent surfaces of the nanocrystalline grains whereas the latter are assigned to their bulk. The residual amorphous matrix was reconstructed in the CEMS/CXMS spectra of the $^{57}Fe_{79}Mo_8Cu_1B_{12}$ alloy by a distribution of quadrupole doublets.

In addition to bcc-Fe phase, presence of Fe_3O_4 (magnetite) was found in the $^{57}Fe_{79}Mo_8Cu_1B_{12}$ alloy annealed at 510 ^{o}C. At the wheel side, it amounted to 12 % and 16 % in the near surface regions (CEMS) and deeper layers (CXMS), respectively. At the air side, the presence of magnetite was confirmed only from the CEMS spectra (ca. 1 %), i.e. very close to the surface regions in the annealed alloy. The corresponding spectral components are plotted in light grey colour in Fig. 2.

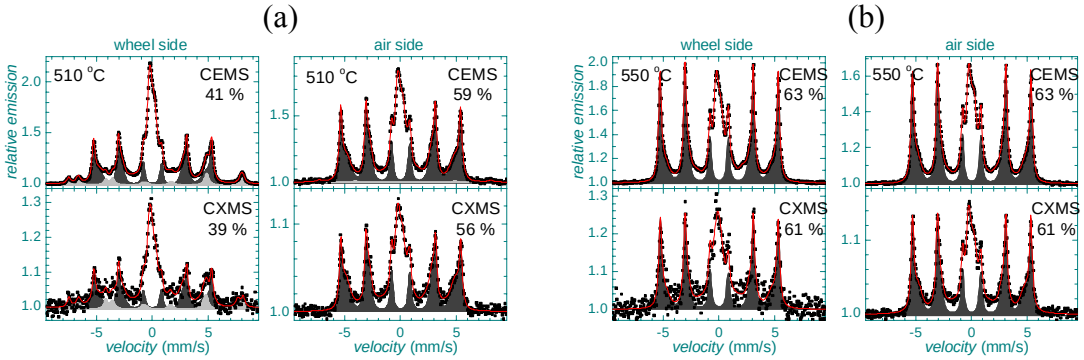

Fig. 2. *CEMS and CXMS spectra for wheel side and air sides of the $^{57}Fe_{79}Mo_8Cu_1B_{12}$ alloy annealed at 510 ^{o}C (a) and 550 ^{o}C (b).*

CEMS and CXMS spectra of the $^{57}Fe_{76}Mo_8Cu_1B_{15}$ alloy are shown in Fig. 3. Amorphous residual matrix was in these spectra refined by distributions of quadrupole doublets and also by distributions of hyperfine magnetic fields. Nevertheless, in contrast to the previous alloy no presence of magnetite was detected either at the wheel or at the air side of the ribbons after annealing at the indicated temperatures. The occurrence of magnetite was found only after annealing up to 450 ^{o}C [2].

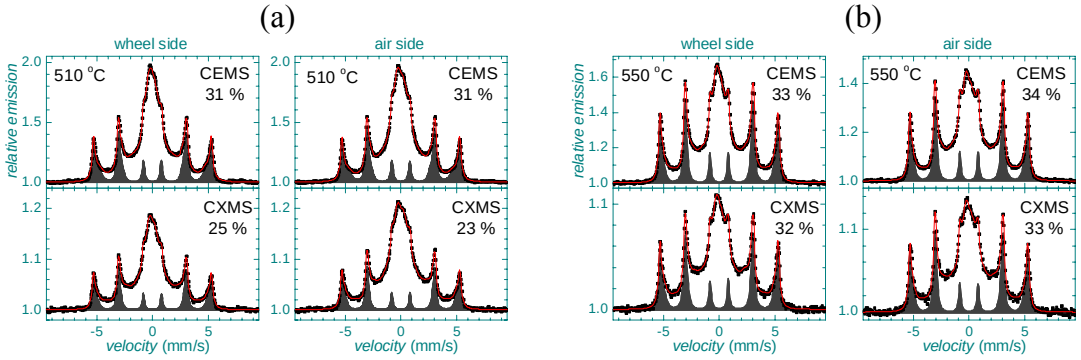

Fig. 3. *CEMS and CXMS spectra for wheel side and air side of the $^{57}Fe_{76}Mo_8Cu_1B_{15}$ alloy annealed at 510 °C (a) and 550 °C (b).*

NIS data were evaluated by the PHOENIX code [3]. Figure 4 shows a density of phonon states (DOS) for the $^{57}Fe_{76}Mo_8Cu_1B_{12}$ and $^{57}Fe_{76}Mo_8Cu_1B_{15}$ alloys.

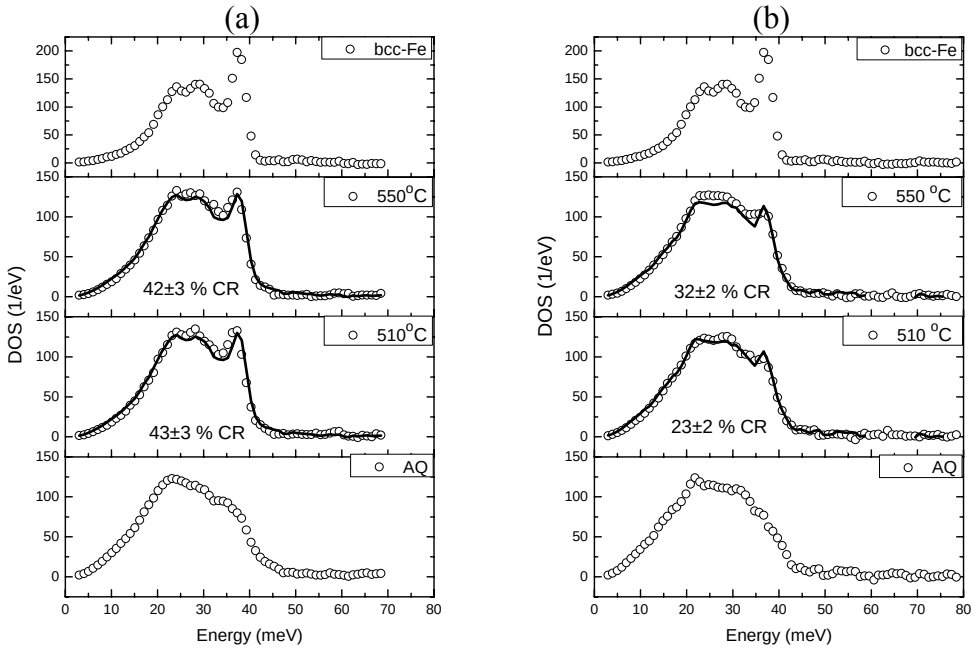

Fig. 4. *DOS for $^{57}Fe_{79}Mo_8Cu_1B_{12}$ (a) and $^{57}Fe_{76}Mo_8Cu_1B_{15}$ (b) alloys.*

DOS of the annealed samples, DOS_{NC} were calculated as a superposition of $DOS_{bcc\text{-}Fe}$ that corresponds to a fully crystalline material (bcc-Fe foil) and DOS_{AM} obtained from our alloys that were measured in the as-quenched state. According to [4], they can be described by the following equation:

$$DOS_{NC} = X_{CR}.(DOS_{bcc-Fe})^{\Gamma} + (1 - X_{CR}).DOS_{AM} \qquad (1)$$

where X_{CR} represents the crystalline fraction and Γ is close to unity. Both X_{CR} and Γ are free parameters. By fitting the free parameters from eq. (1) we have obtained the relative fractions of the nanocrystalline states (X_{CR}) and the theoretical dependences of DOS which are plotted in Fig. 4 by solid lines.

In Table 1, the relative fractions of bcc-Fe nanocrystalline phase obtained from CEMS, CXMS, and NIS measurements are compared for the $^{57}Fe_{79}Mo_8Cu_1B_{12}$ and $^{57}Fe_{76}Mo_8Cu_1B_{15}$ alloys. Surface crystallization in the $^{57}Fe_{76}Mo_8Cu_1B_{15}$ alloy derived from CEMS experiments is almost the same at both sides of the ribbon. Slightly higher amount of bcc-Fe was found in the sample annealed at 550 ^{o}C. Subsurface regions scanned by CXMS exhibit smaller amounts of bcc-Fe especially in the alloy annealed at 510 ^{o}C. For both temperatures, these values are close to the bulk ones obtained from NIS experiments.

In case of the $^{57}Fe_{79}Mo_8Cu_1B_{12}$ alloy the differences between relative iron contents derived from CEMS/CXMS and NIS measurements are more pronounced. Data obtained from CEMS and diffraction of synchrotron radiation (DSR) for this alloy show in the as-quenched state surface crystallization of about 10 % [5]. This was not accounted for in the evaluation of the DOS_{NC} according to eq. (1) because the corresponding DOS_{AM} was supposed to be fully amorphous. Correction of the DOS_{NC} by 10 % in as-quenched state is included in the Table 1.

Tab. 1. *Relative fractions of bcc-Fe nanocrystalline phase obtained from CEMS, CXMS, and NIS measurements*.

Technique/ Alloy	$^{57}Fe_{79}Mo_8Cu_1B_{12}$				$^{57}Fe_{76}Mo_8Cu_1B_{15}$			
	510 ˚C		550 ˚C		510 ˚C		550 ˚C	
	Wheel	Air	Wheel	Air	Wheel	Air	Wheel	Air
CEMS	41 %	59 %	63 %	63 %	31 %	31 %	33 %	34 %
CXMS	39 %	56 %	61 %	61 %	25 %	23 %	32 %	33 %
NIS	43 %		42 %		23 %		32 %	
NIS-corr.	53 %		52 %		-		-	

4. Conclusion

We have investigated the formation of crystalline phases in the $^{57}Fe_{79}Mo_8Cu_1B_{12}$ and $^{57}Fe_{76}Mo_8Cu_1B_{15}$ alloys by CEMS, CXMS, and NIS techniques. From CEMS/CXMS, we obtained information about surface crystallization. Bulk crystallization was assessed from the results of NIS. Table 1 compares the relative fractions of nanocrystalline bcc-Fe as obtained for CEMS, CXMS, and NIS measurements. In addition to bcc-Fe, presence of magnetite was revealed by CEMS and CXMS in the $^{57}Fe_{79}Mo_8Cu_1B_{12}$ alloy on its wheel side.

Acknowledgement

This work was supported by the grants VEGA 1/0286/12 and SK-PL-0032-12 and it was performed as a part of the IAEA RC-1196.1 action entitled ‘Utilisation of accelerator-based real-time methods in investigation of materials with high technological importance’.

References:

[1] M. E. Mchenry, D. E. Willard, D. E. Laughlin, Prog. Mat. Sci., **44**, (1999) 291.
[2] M. Miglierini, T. Hatala, J. Frydrych, K. Šafářová, Hyp. Int., 205 (2012) 125.
[3] W. Sturhahn, Hyp. Int., **125** (2000) 149.
[4] L. Pasquini et. al., Phys. Rev. B **66** (2002) 073410.
[5] T. Hatala, M. Miglierini, Acta Physica Pol. A **118** (2010) 764